Structure and ESR Features of Glycine Radical

Vincenzo Barone,*,† Carlo Adamo,‡ Andre Grand,§ Frank Jolibois,§ Yvon Brunel,⊥ and Robert Subra⊥

Contribution from the Dipartimento di Chimica, Università Federico II, via Mezzocannone 4, I-80134 Napoli, Italy, Dipartimento di Chimica, Università della Basilicata, via Nazario Sauro 85, I-85100 Potenza, Italy, Service d'Etudes des Systémes et Architectures Moléculaires (SESAM), DRFMC, CEN Grenoble, BP 85X, F-38041 Grenoble Cédex, France, and Laboratoire d'Etudes Dynamiques et Structurales de la Séléctivité (LEDSS), Université Joseph Fourier, 301 Avenue de la Chimie, BP 53X, F-38041 Grenoble Cédex, France

Received June 30, 1995⊗

Abstract: The structure, conformational behavior, and ESR features of the glycine radical have been investigated by an established quantum-mechanical protocol with the aim of better elucidating the role of intrinsic and environmental effects in determining the physicochemical properties of amino acid radicals involved in biological systems. From a structural point of view, extraction of a hydrogen atom from glycine modifies only the local environment of the C^{α} atom. The conformational freedom of the radical is, however, severely restricted with respect to its closed-shell parent. In particular, only planar or nearly planar structures are energetically accessible. These are characterized by very similar hyperfine splittings, which are in agreement with experiment for C^{α} and N, but are significantly too large for H^{α}. Although the average value of H(N) splittings is not far from the experimental value, the two protons are strongly not equivalent. The computed torsional barrier around the $N-C^{\alpha}$ bond is too high to allow an effective rotational averaging and also inversion of the NH_2 moiety, which is governed by a low-energy barrier (≈3 kJ/mol), cannot restore agreement with experiment. Inclusion of solvent-induced structural modifications significantly improves matters for H^{α}, whereas the equivalence of H(N) atoms in acidic solution can be explained in terms of a mixture between the neutral species and a nonclassical cationic form.

1. Introduction

During the past few years, the interest for protein radicals has considerably increased and glycine radicals[1] engaged in peptidic chains have been recently identified by electronic spin resonance (ESR) spectroscopy.[2,3] A first theoretical investigation of the so-called dipeptide analogue of the glycine radical has given satisfactory results,[4] but there is a need for more systematic theoretical studies of the structures and ESR parameters of radicals derived from amino acids and peptides. The ESR parameters of amino acid radicals in aqueous solution have been experimentally studied by a number of groups using continuous-flow methods.[5−13] Among these the simple carbon-centered glycine radical, $H_2N-CH-COOH$, plays a prominent role[1−4] and has been carefully characterized in a recent study from a thermochemical point of view.[5] However, its structure in aqueous solution has been, in the past, a subject of controversy, some authors postulating that the radical might be more stable in its zwitterionic form ($H_3N^+-CH-COO^-$),[6] the others favoring the molecular form in acidic or neutral solutions, and the anionic radical $[H_2N-CH-COO]^-$ in basic aqueous solutions.[8] Furthermore, some investigations of the radical in the solid state unambiguously identified the zwitterionic form.[14−16] It must be noticed that the parent glycine molecule prefers a zwitterionic form in the solid state,[17] while the covalent form H_2N-CH_2-COOH is more stable in the gas phase.[18−25] Nevertheless, if one compares the H^{α} isotropic hyperfine splittings of the glycine radical, in either its neutral or anionic forms, with those obtained for a series of other amino acids,[7] one observes a striking difference. As a matter of fact the splitting of H^{α} is always around 20 G, while in the glycine radical it is as low as 12 G. Furthermore, the H^{α} of the zwitterionic form of the glycine radical in the solid state has a more usual splitting of 26.8 G.[14] The "anomalous" coupling

† Università Federico II.
‡ Università della Basilicata.
§ Service d'Etudes des Systémes et Architectures Moléculaires.
⊥ Laboratoire d'Etudes Dynamiques et Structurales de la Séléctivité.
⊗ Abstract published in *Advance ACS Abstracts*, December 1, 1995.

(1) (a) Hayon, E.; Simic, M. *J. Am. Chem. Soc.* **1971**, *93*, 6781. (b) Kirino, Y.; Taniguchi, H. *J. Am. Chem. Soc.* **1976**, *98*, 5089.
(2) Volker, V.; Wagner, A. F.; Frey, M.; Neugerbauer, F. A.; Schafer, W.; Knappe, J. *Proc. Natl. Acad. Sci. U.S.A.* **1992**, *89*, 996.
(3) Mulliez, E.; Fontecave. M.; Gaillard, J.; Reichard, P. *J. Biol. Chem.* **1993**, *268*, 2296.
(4) Barone, V.; Adamo, C.; Grand, A.; Brunel, Y.; Fontecave, M.; Subra, R. *J. Am. Chem. Soc.* **1995**, *117*, 1083.
(5) Armstrong, D. A.; Rauk, A.; Yu, D. *J. Chem. Soc., Perkin Trans. II* **1995**, 553.
(6) Armstrong, W. A.; Humphreys, W. J. *Can. J. Chem.* **1967**, *45*, 2589.
(7) Taniguchi, H.; Fukui, K.; Ohnishi, S.; Hatano, H.; Hasegawa, H.; Maruyama, T. *J. Phys. Chem.* **1968**, *72*, 1925.
(8) Smith, P.; Fox, W. M.; McGintry, D. J.; Stevens, R. D. *Can. J. Chem.* **1970**, *48*, 480.
(9) Neta, P.; Fessenden, R. W. *J. Phys. Chem.* **1971**, *75*, 738.
(10) Box, H. C.; Budzenski, E. E.; Lilga, K. T. *J. Chem. Phys.* **1972**, *57*, 4295.
(11) Sinclair, J.; Codella, P. *J. Chem. Phys.* **1972**, *59*, 1569.
(12) Moriya, F.; Makino, K.; Suzuki, N.; Rokushika, S.; Hatano, H. *J. Phys. Chem.* **1980**, *84*, 3085.
(13) Legasov, V. A.; Usatyi, A. F.; Ibragimov, R. A.; Myasoodov, N. F. *J. Chem. Phys.* **1982**, *76*, 91.
(14) Ghosh, D. K.; Whiffen, V. H. *Mol. Phys.* **1959**, *2*, 285.
(15) Weimer, R. F.; Koski, W. S. *J. Am. Chem. Soc.* **1963**, *85*, 873.
(16) Morton, J. R. *J. Am. Chem. Soc.* **1964**, *86*, 2325.
(17) Nunone, K.; Muto, H.; Toriyama, K.; Iwasaki, M. *J. Chem. Phys.* **1976**, *65*, 3805.
(18) Almlof, J.; Kuick, A.; Thomas, J. O. *J. Chem. Phys.* **1973**, *59*, 3901.
(19) Frey, R. F.; Coffin, J.; Newton, S. Q.; Ramek, M.; Cheng, V. K. W.; Momany, F. A.; Schaffer, L. *J. Am. Chem. Soc.* **1992**, *114*, 5369.
(20) Csazar, A. J. *J. Am. Chem. Soc.* **1992**, *114*, 9568.
(21) Hu, C.; Shen, M.; Schaffer, H. F., III *J. Am. Chem. Soc.* **1993**, *115*, 2923.
(22) Lelj, F.; Adamo, C.; Barone, V. *Chem. Phys. Lett.* **1994**, *230*, 189.
(23) Barone, V.; Adamo, C.; Lelj, F. *J. Chem. Phys.* **1995**, *101*, 366.
(24) Yu, D.; Rauk, A.; Armstrong, D. A. *J. Am. Chem. Soc.* **1995**, *117*, 1789.
(25) Godfrey, P. D.; Brown, R. D. *J. Am. Chem. Soc.* **1995**, *117*, 2019.

0002-7863/95/1517-12618$09.00/0

of H^{α} in aqueous solution raises the problem of the electronic structure of the radical and of the corresponding ESR features.

Isotropic hyperfine splittings of free radicals provide a severe challenge to theoretical chemistry, since they are related to subtle details of the ground state electronic wave function. This has stimulated much work, and the most sophisticated post-Hartree–Fock (especially coupled clusters[26,27] or multireference configuration interaction[28–30]) and density functional[31] models are providing wave functions of sufficient quality. However, the first class of methods is too expensive for systematic studies of large molecules, and the second class is still not sufficiently tested. Recent studies have shown that, at least for carbon-centered π and quasi-π radicals, wave functions obtained by low-order perturbative correlation treatments give expectation values of the spin density at nuclei close to those obtained by more sophisticated approaches.[26,32,33] Although this would define, in principle, a viable strategy for electronic computations, the reliability of hyperfine couplings obtained at this level has been recently questioned.[28] We have, therefore, performed some test computations with larger basis sets and more complete inclusion of correlation energy.

From another point of view, vibrational averaging of the hyperfine coupling constants by large-amplitude inversion motions at the radical center sometimes can be very important: for instance the isotropic hyperfine splitting of ^{13}C in the methyl radical is enhanced by about 30% by vibrational averaging.[32] We have recently shown that the combined use of correlated electronic wave functions with medium-size basis sets and proper account of vibrational modulation effects through effective large-amplitude nuclear Hamiltonians provides a powerful and reliable tool to investigate ESR features of flexible radicals.[32,34] Here we apply this general quantum mechanical protocol to a comprehensive study of the conformational behavior and magnetic properties of the glycine radical.

Finally a systematic study of solvent effects would require the combined use of quantum-chemical and statistical (e.g. molecular dynamics) techniques. Pending this analysis, we report here some preliminary results obtained through geometry optimization of small glycine–water clusters by a density functional approach.

2. Computational Methods

Electronic computations have been performed with the GAUSSIAN/92[35] and DGAUSS[36] codes running on the C94 Cray computer at the CEA-CEN Grenoble and on RS-6000 workstations at the University of Naples. Vibrational effects have been computed by the DiNa package.[34,37]

Density functional (DF) computations were performed within the unrestricted Kohn–Sham (UKS) formalism using the so-called VWN local functional,[38] a polarized split valence orbital basis set (DZVP)[39] especially optimized for DF computations, and a (7/3/3;7/3/3) auxiliary basis set (A1).[40]

Hartree–Fock wave functions were generated by the Unrestricted (UHF) formalism, correlation energy being then introduced by many-body perturbation theory employing the Møller–Plesset Hamiltonian partitioning[41] carried up to second order (UMP2) or by the so-called quadratic configuration interaction approach including single and double excitations (UQCISD) and, in some cases, a perturbative estimate of triples (UQCISD[T]).[42]

Although the wave function consisting of UHF orbitals does not represent a correct spin state, all the computations reported in the present study give $0.75 < S^2 < 0.78$ and annihilation of the quartet contribution leaves essentially no residual spin contamination ($S^2 < 0.751$). In such circumstances we can expect good structures and spin-dependent properties from unrestricted computations.

A full double-ζ polarized basis set is the smallest reasonable set for determination of hyperfine parameters, since each highly occupied orbital requires a partner spin polarization orbital which is localized in roughly the same region of space, but is typically a little more diffuse. Although not all double-ζ and larger bases provide satisfactory results, one that does is Dunning's [4,2;2] contraction of the Huzinaga (9s,5p;4s) basis.[43a] When augmented by single polarization functions on all atoms,[43b] this basis set, hereafter referred to as DZP, has been our standard for the computation of spin-dependent properties. Some computations also have been performed by the (10,6,1;5,1)/[6,4,1;3,1] basis set introduced by Chipman[44] and further validated in ref 32b (referred to as the TZP^{+} basis set).

The structures of the most significant conformers have been fully optimized by gradient methods at the UMP2/DZP level. More reliable energy differences and spin-dependent properties have been obtained by single-point UQCISD/DZP and UQCISD/TZP^{+} computations at the above geometries.

The formulae for calculating hyperfine parameters are obtained from the spin Hamiltonian,[45]

$$H_{spin} = -g\beta S_z B_z - g_N \beta_N I_z \beta_z + S.A.I$$

The first two contributions are the electronic and nuclear Zeeman terms, respectively, and arise from the interactions between a magnetic field B and the magnetic moments of the unpaired electrons (S_z) or the magnetic nuclei (I_z) in the system. The remainder is the hyperfine term, and is a result of the interactions between the unpaired electrons and the nuclei. β_e and β_N are the electron and nuclear magnetons, and g_N is the nuclear magnetogyric ratio.

The 3×3 hyperfine interaction tensor **A** can be further separated into its isotropic (spherically symmetric) and anisotropic (dipolar) components. Isotropic hyperfine splittings a_N in MHz are related to the spin densities $\rho^{\beta}(\mathbf{r}_N)$ at the corresponding nuclei by

(26) (a) Sekino, H.; Bartlett, R. J. *J. Chem. Phys.* **1985**, *82*, 4225. (b) Pereira, S. A.; Watts, J. D.; Bartlett, R. J. *J. Chem. Phys.* **1994**, *100*, 1425.
(27) Carmichael, I. *J. Phys. Chem.* **1991**, *95*, 6198.
(28) Feller, D.; Glendening, E. D.; McCullough, E. A., Jr.; Miller, R. J. *J. Chem. Phys.* **1993**, *99*, 2829.
(29) Fernández, B.; Jørgensen, P.; McCullough, E. A., Jr.; Symons, J. *J. Chem. Phys.* **1993**, *99*, 5995.
(30) (a) Engels, B. *J. Chem. Phys.* **1994**, *100*, 1380. (b) Suter, H. U.; Engels, B. *J. Chem. Phys.* **1994**, *100*, 2936.
(31) (a) Barone, V.; Adamo, C.; Russo, N. *Chem. Phys. Lett.* **1993**, *212*, 5. (b) Barone, V. *Chem. Phys. Lett.* **1994**, *226*, 392. (c) Barone, V. *J. Chem. Phys.* **1994**, *101*, 6834. (d) Barone, V. *J. Chem. Phys.* **1994**, *101*, 10666. (e) Adamo, C.; Barone, V.; Fortunelli, A. *J. Chem. Phys.* **1995**, *102*, 384.
(32) (a) Barone, V.; Minichino, C.; Faucher, H.; Subra, R.; Grand, A. *Chem. Phys. Lett.* **1993**, *205*, 324. (b) Barone, V.; Minichino, C.; Grand, A.; Subra, R. *J. Chem. Phys.* **1993**, *99*, 6787. (c) Barone, V.; Grand, A.; Minichino, C.; Subra, R. *J. Phys. Chem.* **1993**, *97*, 6355.
(33) (a) Cramer, C. J. *J. Am. Chem. Soc.* **1991**, *113*, 2439. (b) Cramer, C. J. *Chem. Phys. Lett.* **1993**, *202*, 297. (c) Cramer, C. J.; Lim, M. H. *J. Phys. Chem.* **1994**, *98*, 5024.
(34) (a) Minichino, C.; Barone, V. *J. Chem. Phys.* **1994**, *100*, 3717. (b) Barone, V.; Minichino, C. *Theochem.* **1995**, *330*, 325.
(35) Frisch, M. J.; Trucks, G. W.; Head-Gordon, M.; Gill, P. M. W.; Wong, M. W.; Foresman, J. B.; Johnson, B. G.; Schlegel, H. B.; Robb, M. A.; Replogle, E. S.; Gomperts, R.; Andres, J. L.; Raghavachari, K.; Binkley, J. S.; Gonzalez, C.; Martin, R. L.; Fox, D. J.; DeFrees, D. J.; Baker, J.; Stewart, J. J. P.; Pople, J. A. GAUSSIAN92; Gaussian Inc.: Pittsburgh, PA, **1992**.
(36) Andzelm, J.; Wimmer, E. *J. Chem. Phys.* **1992**, *96*, 1280.
(37) Barone, V.; Jensen, P.; Minichino, C. *J. Mol. Spectrosc.* **1992**, *154*, 252.
(38) Vosko, S.; Wilk, L.; Nusair, M. *Can. J. Phys.* **1980**, *58*, 1200.
(39) Andzelm, J.; Radzio, E.; Salahub, D. R. *J. Comput. Chem.* **1988**, *6*, 520.
(40) Godbout, R.; Salahub, D. R.; Andzelm, J.; Wimmer, E. *Can. J. Chem.* **1992**, *70*, 560.
(41) Moller, C.; Plesset, M. S. *Phys. Rev.* **1934**, *46*, 618.
(42) Pople, J. A.; Head-Gordon, M.; Raghavachari, K. *J. Chem. Phys.* **1987**, *87*, 5968.
(43) (a) Dunning, T. H., Jr. *J. Chem. Phys.* **1970**, *53*, 2823. (b) Dunning, T. H., Jr.; Hay, P. J. In *Modern Theoretical Chemistry*; Schaefer, H. F., III, Ed.; Plenum Press: New York, 1977; Vol. 2, Chapter 1.
(44) Chipman, D. M. *Theor. Chim. Acta* **1989**, *76*, 73. Chipman, D. M. *J. Chem. Phys.* **1989**, *91*, 5455.
(45) Weltner, W., Jr. *Magnetic Atoms and Molecules*; van Nostrand: New York, 1983.

$$a_N = \frac{8\pi}{3}\beta_e g_N \beta_N \sum_{\mu,\nu} P^{\alpha-\beta}_{\mu,\nu} \langle \varphi_\mu | \delta(\mathbf{r}_{kN}) | \varphi_\nu \rangle$$

The splittings are usually given in units of MHz by microwave spectroscopists and in gauss (1 G = 0.1 mT) by ESR spectroscopists. In the present work all the values are given in gauss and assuming that the free electron g value is appropriate also for the radicals. To convert data to MHz one has to multiply by 2.8025.

The study of large-amplitude vibrations requires, especially in the case of large molecules, some separation between the active large-amplitude motion (LAM) and the *spectator* small-amplitude modes (SAM). If the LAM occurs along the steepest descent path in the mass weighted coordinate space (the so-called intrinsic large-amplitude path, ILAP[46]) the gradient is parallel to the path so that first-order potential couplings between LAM and SAM's disappear.[47] For intramolecular dynamics, however, the simpler distinguished coordinate (DC) approach has the advantage of being invariant upon isotopic substitutions and also well-defined beyond energy minima. This model corresponds to the construction of the one-dimensional path through the optimization of all the other geometrical parameters at selected values of a specific internal coordinate.

When the ILAP is traced, successive points are obtained following the energy gradient. Because there is no external force or torque, the path is irrotational and leaves the center of mass fixed.[47] Successive points coming from separate geometry optimizations (as is the case for the DC model) introduce the additional problem of their relative orientation. In fact, the distance in mass weighted Cartesian coordinates between adjacent points is altered by the rotation or translation of their respective reference axes. The problem of translations has the trivial solution of centering the reference axes at the center of mass of the system. On the other hand, for nonplanar systems, the problem of rotations does not have an analytical solution and must be solved by numerical minimization of the distance between successive points as a function of the Euler angles of the system.[48]

When the coupling terms are negligible, the adiabatic Hamiltonian governing the motion along the large-amplitude path assumes the simple form:

$$H(s,n) = \frac{1}{2}p_f^2 + V_{ad}(s,n)$$

where

$$V_{ad}(s,n) = V_0(s) - V_0(s^0) + \hbar \sum_{i=1}^{f-1} \left(n_i + \frac{1}{2}\right)(\omega_i(s) - \omega_i(s^0))$$

$\omega_i(s)$ are the harmonic frequencies of SAM as a function of the large-amplitude coordinate, and s^0 refers to a suitable reference structure lying on the path. The adiabatic potential obtained when all the corresponding quantum numbers are 0 is usually referred to as ground state vibrationally adiabatic potential ($V_{gs}(s)$). If, further, the vibrational frequencies of SAM's do not vary very much along the path, the motion along the LAP is governed by the bare potential $V_0(s)$.

The successive step consists of determining vibrational eigenvalues and eigenfunctions. Local basis set methods are tailored to this end since they give reliable results independently on the shape of the profile. Cubic splines were used to interpolate the potential along the LAP and to generate a larger set of equispaced points on which cubic splines were used as basis functions.[46] The expectation value $\langle O \rangle_j$ of a given observable in the vibrational eigenstate $|j\rangle$ corresponding to the eigenvalue ϵ_j is given by:

$$\langle O \rangle_j = O_{ref} + \langle j(s) | \Delta O(s) | j(s) \rangle$$

where O_{ref} is the value of the observable at the reference configuration,

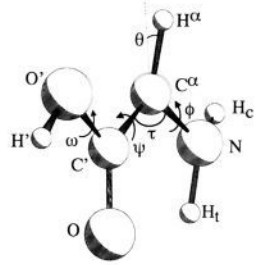

Figure 1. Structure and atom labeling for the carbon-centered glycine radical. The conformation shown in the figure corresponds to $\phi = \psi = \omega = 0°$.

and $\Delta O(s)$ is the expression (here a spline fit) giving its variation as a function of the progress variable s. The temperature dependence of the observable is obtained by assuming a Boltzmann population of the vibrational levels, so that:

$$\langle O \rangle_T = O_{ref} + \frac{\sum_{j=0}^{\infty} \langle j | \Delta O | j \rangle \exp[(\epsilon_0 - \epsilon_j)/KT]}{\sum_{j=0}^{\infty} \exp[(\epsilon_0 - \epsilon j)/KT]}$$

The above equations point out the possibility of computing the reference value of the observable at a very sophisticated level (UQCISD/TZP+ in our protocol) and vibrational averaging effects at a lower level (UMP2/DZP in our protocol).

3. Results and Discussion

Recent studies of the structures and stabilities of all the possible radicals derived from H atom extraction from glycine (N-centered, O-centered, and C-centered) concluded that C-centered radicals are significantly more stable.[24] As a consequence we will consider in the following only this family of radicals (see Figure 1).

3.1 Geometric Structure and Conformational Behavior. In its neutral form, the C-centered glycine radical has three internal rotational degrees of freedom (ϕ, ψ, and ω), associated with C−N (ϕ), C−C (ψ), and C−O (ω) bonds, respectively (see Figure 1). However, the only values allowed for ω are 0° and 180°. On the other hand, unsymmetrical structures derived from small deformations of symmetric limiting models also must be taken into account.

The conformational behavior of glycine radical is well evidenced by the , ψ map of Figure 2 for $\omega = 0°$. A very similar map is obtained for $\omega = 180°$. The most striking feature of these maps is the presence of energy minima only for planar or nearly planar arrangements of the whole molecule. They will be referred to as **I** (ϕ,ψ,ω = 0°,0°,0° or 180°,0°,0°), **II** (ϕ,ψ,ω = 0°,180°,0° or 180°,180°,0°), **III** (ϕ,ψ,ω = 0°,0°,180° or 180°,0°,180°), and **IV** (ϕ,ψ,ω = 0°,180°,180° or 180°,180°,180°). Starting from these structures, full geometry optimization leads to the unsymmetrical energy minima reported in Table 1. At the UMP2/DZP level the energy differences from the most stable structure **I** are 9.2 (**II**), 38.7 (**III**), and 51.2 (**IV**) kJ mol^{-1}. This implies that only the first two conformers can be significantly populated at not too high temperature. As a consequence we will consider in the following only structures **I** and **II**. UQCISD/DZP single-point computations at the above geometries reduce the energy difference to 5.6 kJ mol^{-1}, in good agreement with the value (5.8 kJ mol^{-1}) recently obtained by the comparable G2 procedure.[24]

(46) Fukui, K. *J. Phys. Chem.* **1970**, *74*, 4161. Fukui, K. *Acc. Chem. Res.* **1981**, *14*, 363.
(47) Miller, W. H.; Handy, N. C.; Adams, J. E. *J. Chem. Phys.* **1980**, *72*, 99.
(48) Zhixing, C. *Theor. Chim. Acta* **1989**, *75*, 481.
(49) Cremaschi, P. *Mol. Phys.* **1980**, *40*, 401.

Table 1. Geometry (Å and deg) of Different Conformers of the Glycine Radical and of Different Structures of the Corresponding Cation Radical from UMP2/DZP Computations

parameter	I	II	III	IV	$[H_3NCHCOOH]^+$	$[H_2NCHC(OH)_2]^+$
$C^\alpha-N$	1.365	1.369	1.364	1.393	1.459	1.341
$N-H_c$	1.007	1.007	1.007	1.010	1.028	1.011
$N-H_t$	1.012	1.009	1.013	1.014	1.052	1.013
$C^\alpha-C'$	1.443	1.446	1.459	1.477	1.514	1.410
$C'-O'$	1.363	1.376	1.365	1.368	1.316	1.318
$O'-H$	0.971	0.971	0.967	0.970	0.972	0.972
$C'-O$	1.234	1.224	1.222	1.208	1.213	1.324
$C^\alpha-H^\alpha$	1.078	1.078	1.080	1.079	1.081	1.081
$O-H$						0.972
H_c-N-C^α	119.7	118.4	120.2	114.5	113.1	120.2
H_t-N-C^α	117.5	116.2	117.9	115.2	109.8	121.4
H_c-N-H_t	115.1	116.9	114.5	111.1		118.3
$C^\alpha-C'-O'$	112.8	111.1	116.6	113.8	118.7	117.6
$C'-O'-H$	104.7	104.5	109.5	108.2	113.8	115.0
$O-C'-O'$	122.8	122.2	120.9	121.6	124.7	115.2
$C'-O-H$						124.8
τ	117.2	121.7	115.9	114.0	109.0	121.1
ω	179.3	−179.4	−1.9	16.4	0.0	179.7
θ	4.8	1.7	2.8	24.2	−3.4	3.9
ϕ	150.4	154.3	152.2	139.6	4.2	175.5
ψ	−172.7	4.3	5.1	54.0	175.9	175.5
ΔE	0.0[a]	9.2[a], 5.6[b]	38.7[a]	51.2[a]	18.3[c]	0.0[c]

[a] With respect to conformer **I**, whose total energy is −283.13489 au at the UMP2/DZP level and −283.17073 au at the UQCISD/DZP//UMP2/DZP level. [b] UQCISD/DZP at UMP2/DZP geometry. [c] With respect to $[H_2NCHC(OH)_2]^+$, whose total energy is −283.39636 au at the UMP2/DZP level.

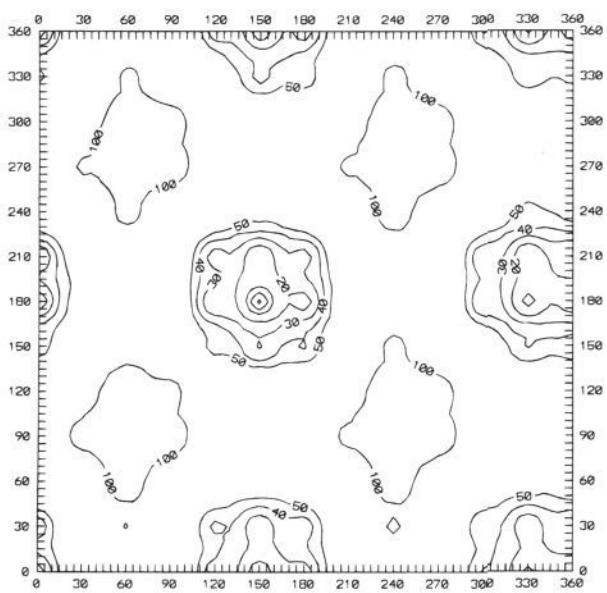

Figure 2. Rigid rotor (ϕ,ψ) map for the glycine radical (with $\omega = 0°$) obtained by UMP2/DZP computations. Contour lines are drawn every 10 kJ mol^{-1} up to 50 kJ mol^{-1} above the absolute minimum. The contour corresponding to 100 kJ mol^{-1} is also shown.

In all cases the NH_2 moiety remains slightly pyramidal (the sum of valence angles around N is 353° in **I** versus 326° in the analogous conformation of glycine) and the radical center is slightly bent. It is noteworthy that H^α and HN hydrogens are always on opposite sides of the mean molecular plane (see Figure 3).

These conformational features are, of course, related to the replacement of the sp^3 C^α atom of glycine by a nearly sp^2 radical center, which allows an effective electron delocalization along the whole structure. This induces, in turn, a greater resistence to any deformation destroying the planarity of the system. The same effect has been previously invoked to explain the stability of the $NH_2CHCOOH$ tautomeric form in acidic aqueous solutions.[8] Further support to this interpretation is given by the structural parameters of Table 1. They clearly show that

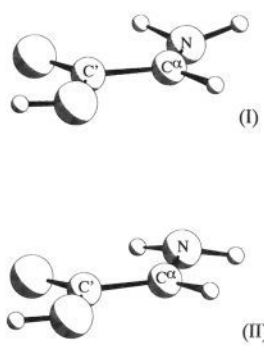

Figure 3. Perspective drawing of the UMP2/DZP optimized structures for conformers **I** and **II** of the carbon-centered glycine radical.

the only significant differences between the radical and the parent molecule concern the local environment of the C^α atom: in the radical the $NC^\alpha C'$ angle (τ) increases and the NC^α, $C^\alpha C'$ bond lengths decrease.

3.2. ESR Features. The ESR spectrum obtained at pH = 1 after hydrogen abstraction from the substrate glycine at 25 °C within an aqueous continuous-flow system using the titanous chloride−hydrogen peroxide radical-generating method[9] shows a doublet (1:1) (11.77 G) of triplets (1:1:1) (6.38 G) of triplets (1:2:1) (5.59 G). This spectrum has been attributed to the radical $H_2N-CH-COOH$ with the following assignment: $|a_H^{CH}| = 11.77\ G$; $|a_N| = 6.38\ G$; $|a_H^{NH_2}| = 5.59\ G$. Note that only absolute values of isotropic hyperfine splittings are available from experiment.

The presence of two equivalent NH protons has been confirmed by an ESR experiment performed in a D_2O solution.[9] As expected for two deuterium nuclei, in such conditions the proton triplets at 5.59 G were replaced by quintets at 0.87 G. During this experiment the H^α hfs was slightly modified (12.00 vs 11.77 G in aqueous solution), indicating a minor change of the hydrogen spin density under the influence of the solvent.

As a first step we have computed the isotropic hyperfine splittings of the four stable conformers of glycine radical at the UMP2/DZP and UQCISD/DZP levels using the optimized UMP2/DZP geometries discussed above (Table 2). The results

Table 2. Isotropic Hyperfine Splittings (in Gauss) for Different Conformers of the Glycine Radical Obtained by UMP2/DZP and UQCISD/DZP Computations at UMP2/DZP Geometries (See Table 1)[a]

	I		II		III	IV
	UMP2	UQCISD	UMP2	UQCISD	UMP2	UMP2
C^α	4.0	13.4	4.5	14.7	3.3	15.4
N	8.1	7.0	8.2	7.0	8.6	5.4
H_c	−3.8	−2.8	−3.7	−2.6	−4.4	−6.6
H_t	−7.1	−6.0	−5.9	−4.8	−8.0	16.0
C′	1.4	−13.1	4.8	−14.1	6.9	10.4
H′	−2.5	−1.8	−1.9	−1.0	−1.9	0.1
H^α	−15.7	−18.9	−16.3	−18.9	−15.5	−20.9

[a] All the electrons have been considered in the correlation treatments. The atom labeling is given in Figure 1.

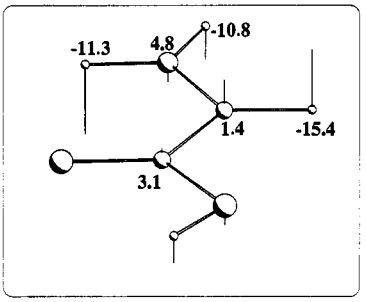

Figure 4. Perspective drawing of the C_s first-order saddle point obtained at the UMP2/DZP level. The composition of the transition vector and the hfs on different atoms (in G) are also indicated.

obtained by the two sets of computations are quite similar, except for the carbon atoms, whose hyperfine splittings are more than doubled at the UQCISD level. Furthermore, the splittings of the different conformers are so similar that we performed further tests (extension of the basis set, vibrational averaging) only for the most stable conformer (**I**). The results of Table 3 show that the computed values are relatively stable upon inclusion of core electrons in the correlation treatment and further extension of the basis set above the DZP level.

Coming to the vibrational treatment, we recall that, among low-frequency vibrations, usually only those corresponding to hindered rotations or inversion motions involving the radical center have a significant effect on ESR parameters. As mentioned in the preceding section, internal rotations are severely restricted in this radical (see Figure 2). On the other hand, the C_s transition state shown in Figure 4 provides a better reference structure for the analysis of inversion motions due to complete separation between in-plane (A′) and out-of-plane (A″) vibrations. Furthermore, it is very close in energy to the pyramidal minimum (ΔE = 3 kJ/mol), and the transition vector leading to the energy minimum (characterized by a very low imaginary frequency of $\approx 300i$ cm^{-1}) involves (albeit with different weights) all the hydrogen atoms. Since other low-frequency A″ normal modes involve the same atoms with different weights we decided to investigate vibrational averaging

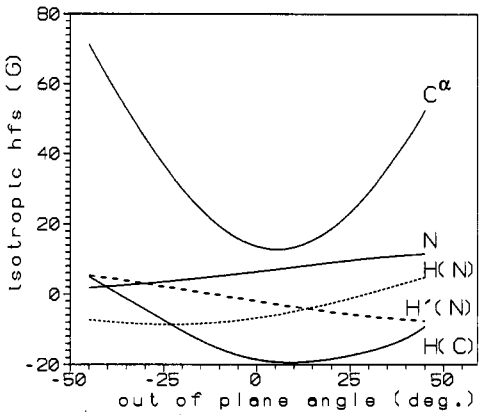

Figure 5. Evolution of isotropic hyperfine couplings as a function of the out-of-plane angle of H^α (θ) for conformer **I** of the glycine radical.

effects performing constrained optimizations for the out-of-plane motion of each hydrogen atom separately. Figure 5 shows, as an example, the evolution of hyperfine splittings connected to the out-of-plane displacement of H^α, when all the other degrees of freedom are optimized for each point. It is quite apparent that only C^α and H^α are significantly affected by this deformation. In particular the splitting of C^α increases sharply with pyramidalization, whereas that of H^α becomes smoothly less negative. This trend can be related to the increase of the positive contribution from delocalization upon pyramidalization, whereas the spin polarization contribution (which is negative for H^α) changes much more slowly. It is noteworthy that the vibrational coorections are essentially identical at the UMP2 and UQCISD levels (Table 4). This confirms the reliability of a cheaper procedure[32] in which only equilibrium values are computed by the expensive UQCISD model, whereas vibrational modulation effects (which require a large number of computations) are computed at the UMP2 level. In an analogous way, out-of-plane motion of H_c only affects the hyperfine splittings of N and H_c and motion of H_t those of N and H_t. It is noteworthy, in this connection, that by increasing the out-of-plane angle of one of the two H(N) atoms, the optimized out-of-plane angle of the other H(N) hydrogen is correspondingly reduced. In any case, the vibrationally averaged splittings of atoms belonging to the NH_2 moiety are very near their equilibrium value.

The above effects lead to the following trends with respect to the experimental ESR spectrum: the agreement for nitrogen is good, the value for the $^{13}C^\alpha$ is in the right range of values (16-21G for glycine engaged in a peptidic chain[2,4]), and the average value for the two H(N) is reasonable. However, the computed values are not compatible with the equivalence between the two protons unambiguously demonstrated by experiments performed in D_2O.[9] Although the two H(N) atoms could become equivalent if the rotation around the NC bond is free or nearly free, this possibility is ruled out by the very high value (~80 kJ/mol) computed for the rotational barrier at any level of theory. Furthermore, the splitting of H^α is too high,

Table 3. Isotropic Hyperfine Splittings (in Gauss) Computed for Conformer **I** of the Carbon-Centered Glycine Radical Using Different Methods and Dielectric Constants in the SCRF Approach

	MP2/DZP[a]		MP2/DZP[b]			QCISD/DZP[a]	QCISD/DZP[b]	QCISD/TZP′[b]
	$\epsilon = 1$	$\epsilon = 78.5$	$\epsilon = 1$	$\epsilon = 78.5$	$\epsilon = 1 + 1H_2O$	$\epsilon = 1$	$\epsilon = 1$	$\epsilon = 1$
C^α	3.4	2.6	4.0	3.2	2.7	12.7	13.4	14.8
H^α	−15.8	−15.1	−15.7	−15.0	−15.3	−18.9	−18.9	−17.9
C′	1.7	0.7	1.4	0.5	2.2	−13.1	−13.1	−13.4
N	8.1	8.3	8.1	8.3	7.8	6.9	7.0	6.6
H_c	−3.6	−3.9	−3.8	−4.1	−3.9	−2.8	−2.8	−2.0
H_t	−7.0	−7.1	−7.1	−7.2	−6.9	−6.0	−6.0	−5.3

[a] Core electrons frozen in the correlation treatment. [b] All electrons included in the correlation treatment.

Table 4. Vibrational Averaging Effects on the Isotropic Hyperfine Splittings (in Gauss) of Conformer **I** Computed at the UMP2/DZP[a] and UQCISD/DZP[b] Levels for Conformer **I** of the Carbon-Centered Glycine Radical[c]

	a_{min}		$\langle\Delta a\rangle$		$\langle a\rangle_{298}$		
	UMP2	UQCISD	UMP2	UQCISD	UMP2	UQCISD	exptl
C^α	4.0	12.8	2.5	2.4	6.5	15.3	
H^α	−15.7	−18.9	0.6	0.6	−15.1	−18.3	11.77
C'	1.4	−13.1	0.2	0.2	1.6	−12.9	
N	8.1	6.9	0.0	0.0	8.1	6.9	6.38
H_c	−3.8	−2.8	0.1	0.1	−3.7	−2.7	5.59
H_t	−7.1	−6.0	0.3	0.3	−6.8	−5.8	5.59

[a] $\omega = 555\ cm^{-1}$, $\nu = 591\ cm^{-1}$, $(\langle\Delta\theta^2\rangle_{298})^{1/2} = 10.7°$, $\langle\theta\rangle_{298} = 5.2°$. [b] $\omega = 543\ cm^{-1}$, $\nu = 566\ cm^{-1}$, $(\langle\Delta\theta^2\rangle_{298})^{1/2} = 10.5°$, $\langle\theta\rangle_{298} = 4.8°$. [c] All the electrons have been explicitly considered in the correlation treatments.

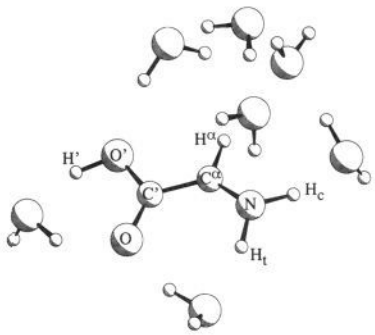

Figure 6. Optimized structure for the adduct of the glycine radical with 7 water molecules.

and the experimental value cannot be approached by adding in the correlation treatment the effect of triple excitations ($\langle a(H^\alpha)\rangle = -17.3$ G at the UQCISD(T)/DZP level) or extending the basis set ($\langle a(H^\alpha)\rangle = -17.5$ G at the UQCISD/TZP$^+$ level).

This situation prompted us to analyze the role played by the solvent in modifying the structure and/or the wave function of the glycine radical. A first investigation has been performed by a simple continuum approach (the so-called SCRF model[50]). Geometry optimization of the radical at the UHF level including the reaction field of the solvent does not introduce any significant change with respect to the isolated radical. As a consequence we have computed the hyperfine splittings at the UMP2/DZP level with the SCRF approach using the corresponding geometric structure optimized in the vacuum. The results of Table 3 show that the solvent reaction field does not alter the trends obtained for the isolated radical, especially concerning the H^α atom. We have next investigated specific solute−solvent effects. In a first step we have optimized the intermolecular parameters of the adduct with a single water molecule with the constraint that the water oxygen atom interacts with the H^α atom. Also in this case the hyperfine splittings of the glycine radical do not show any strong modification. In particular the negligible spin density transfer between the two partners in the adduct is in agreement with the very small modifications observed experimentally when replacing the H_2O solvent by D_2O. It is noteworthy that the slight variations computed for the splittings of C^α and H^α are very similar to those obtained by the continuum approach. We have next performed a full geometry optimization of the system formed by the glycine radical plus seven water molecules (Figure 6) using the DF approach described in the section devoted to computational details. The only significant structural effect

Table 5. Isotropic Hyperfine Splittings (in Gauss) for Different Ionic Forms of the Glycine Radical Obtained from UMP2/DZP and UQCISD/DZP Computations

	$H_3N^+-CH-COO^-$		$[H_3N-CH-COOH]^+$	$[H_2N-CH-C(OH)_2]^+$	
	UMP2	UQCISD	UMP2	UMP2	UQCISD
C^α	35.9	40.0	29.3	2.9	−3.8
C'	−5.0	−13.7	5.2	−6.6	1.5
N	−3.8	−3.8	−3.8	2.4	6.2
H^α	−29.0	−28.4	−30.0	−13.0	−9.4
H_t	−0.1	−0.9	−1.0	−8.8	−12.0
H_c	24.3	25.0	22.7	−8.2	−11.4
$H_{c'}$	24.3	25.0	22.8		

concerns the value of the θ angle, which changes from 5° for the isolated radical to −5° for the adduct with 7 water molecules. Note that this modification corresponds to the passage from a nearly staggered to a nearly eclipsed orientation of $C^\alpha H^\alpha$ and NH bonds. From Figure 5 we see that this change leads to a value of about −15 G for the isotropic hyperfine splitting of H^α, whereas the other splittings are only slightly affected. This shows that this kind of structural modification, if increased up to $\theta = -10°$ under the effect of further solvent molecules, could lead to agreement with experiment. Nevertheless, the equivalence of the two H(N) protons remains incompatible with the structure computed either in the vacuum or in aqueous solution. It remains to investigate the possibility that the experimental ESR spectrum corresponds to a different radical. The presence of a zwitterionic form can be ruled out on the basis of the good agreement between its computed spectrum and that observed in the solid state.[51] Since experiments were undertaken in acidic solutions, cationic species also need some consideration. Among these, the standard $[H_3NCHCOOH]^+$ form can be excluded since it would involve three equivalent H(N) protons with a computed average splitting (15 G) much larger than the experimental value (5.6 G) (see Table 5). Another cationic species ($[H_2N-CH-C(OH)_2]^+$, see Table 5) obtainable from secondary reactions deserves particular consideration, since it is the most stable cationic form[24] and is characterized by nearly equivalent H(N) atoms and a reasonable value of the splitting at H^α. In particular, a mixture of neutral and cationic forms could satisfactorily explain all the experimental observations.

4. Concluding Remarks

We have performed a comprehensive study of the structure and ESR features of the glycine radical. From a methodological point of view, we have confirmed that our general computational protocol coupling sophisticated post-Hartree−Fock computations to a proper account of vibrational averaging effects is able to provide reliable results for the structure and magnetic properties of medium size radicals. Cheaper MP2 computations with standard polarized basis sets are sufficient to reproduce the effect of vibrational averaging, but sometimes (especially for carbon atoms in the present context) provide unreliable equilibrium values for isotropic hyperfine splittings.

From a conformational point of view, the most striking feature of the glycine radical is the strong preference for planar or quasiplanar conformations, which allows an effective delocalization of π electrons across the whole radical. The isotropic hyperfine splittings of all these energy minima are quite similar and in good agreement with experiment at least for N and the average value of the two H(N). However, the isotropic splitting computed for H^α is significantly too large, and agreement with

(50) Wong, M. W.; Wiberg, K. B.; Frisch, M. *J. Chem. Phys.* **1991**, *95*, 8991.

(51) Barone, V.; Adamo, C.; Grand, A.; Subra, R. *Chem. Phys. Lett.* **1995**, 242, 351.

experiment can be restored only by taking into account solvent-induced structural modifications at the radical center. The equivalence of the two NH protons is not compatible with the high values computed for the rotational barrier around the C^{α}–N bond. Our computations suggest, instead, that the EPR spectrum observed in acidic solutions actually corresponds to a mixture of the neutral form with the most stable cationic species (a nonclassical form obtained by secondary reactions).

As a whole our computations offer an internally consistent and very articulated scenario for the behavior of carbon-centered glycine radicals in aqueous solution and call for further experimental investigations aimed to confirm the contemporary presence of neutral and cationic species in acidic solutions containing glycine radicals.

JA952167B